Real-time optical recording of β_1-adrenergic receptor activation reveals supersensitivity of the Arg389 variant to carvedilol

Francesca Rochais,[1] Jean-Pierre Vilardaga,[2] Viacheslav O. Nikolaev,[2] Moritz Bünemann,[2] Martin J. Lohse,[1,2] and Stefan Engelhardt[1]

[1]Rudolf-Virchow-Center, DFG–Research Center for Experimental Biomedicine, and [2]Institute of Pharmacology and Toxicology, University of Würzburg, Würzburg, Germany.

Antagonists of β-adrenergic receptors (β-ARs) have become a main therapeutic regimen for the treatment of heart failure even though the mechanisms of their beneficial effects are still poorly understood. Here, we used fluorescent resonance energy transfer–based (FRET-based) approaches to directly monitor activation of the β_1-AR and downstream signaling. While the commonly used β-AR antagonists metoprolol, bisoprolol, and carvedilol displayed varying degrees of inverse agonism on the Gly389 variant of the receptor (i.e., actively switching off the β_1-AR), surprisingly, only carvedilol showed very specific and marked inverse agonist effects on the more frequent Arg389 variant. These specific effects of carvedilol on the Arg389 variant of the β_1-AR were also seen for control of beating frequency in rat cardiac myocytes expressing the 2 receptor variants. This FRET sensor permitted direct observation of activation of the β_1-AR in living cells in real time. It revealed that β_1-AR variants dramatically differ in their responses to diverse beta blockers, with possible consequences for their clinical use.

Introduction

Activation of cardiac β-adrenergic receptors (β-AR) by endogenous catecholamines plays a key role in the regulation of cardiac function. The heart contains at least 2 β-AR subtypes, termed β_1-*AR* and β_2-*AR*, and may also contain β_3-ARs (1). Stimulation of the β_1-AR represents the strongest endogenous mechanism for increasing contractility and beating frequency of the mammalian heart (1). In human heart failure, which has become one of the leading causes of death and hospitalization (2), the sympathetic nervous system is chronically activated to overcome the loss of cardiac output (3). While this initially leads to compensation through a short-term increase in cardiac function, chronic stimulation of the cardiac β-AR system contributes to progression of the disease (4, 5). These detrimental effects of chronic β-adrenergic signaling are attributed to the β_1-AR subtype. Transgenic mice with cardiomyocyte-specific expression of the β_1-AR develop progressive cardiac hypertrophy and heart failure in a manner similar to that seen in patients with heart failure (6). Consequently, the development of receptor antagonists (7) has resulted in the single most effective therapeutic regimen to treat heart failure (8).

Several common polymorphisms of the human β_1-AR have been identified. Most importantly, the Arg-Gly polymorphism at amino acid position 389 (9, 10) has been associated with cardiac disease (11). Position 389 is located near the seventh transmembrane domain of the receptor in the cytoplasmic tail, within a putative Gs protein–binding domain, corresponding to helix 8 in rhodopsin (12–14). In vitro experiments indicated greater stimulation of adenylyl cyclase activity through the Arg389 variant of the β_1-AR (10). Recent studies showed that the Arg389 polymorphism is associated with a poor prognosis in heart failure (15) and predisposes to hypertension (16). Moreover, patients carrying both the Arg389 variant of the β_1-AR and a deletion variant of the presynaptic α_{2c}-AR receptor had a greatly enhanced risk of developing heart failure (11).

While all these data confirm the concept that chronic β_1-AR signaling is detrimental, it is currently unclear how patients with an inherently hyperfunctional β-AR system should be treated and what substances are effective.

Contradictory results have been reported regarding whether the 389 polymorphism determines the sensitivity of the response to beta blocker treatment (for reviews, see refs. 17–19). While some studies found that the presence of the Arg389 allele of the β_1-AR is associated with a greater heart rate or blood pressure response to beta blockers (15, 20–24), others found no association (25–27). These discrepancies may be attributed to the relatively small sizes of the cohorts and the complex and highly regulated physiological parameters that were studied.

To overcome these limitations, we developed a fluorescent resonance energy transfer (FRET) approach to record directly and in real time the conformational changes of the receptor protein that lead to its activation. Based on the resonance energy transfer between fluorophores of overlapping emission spectra, FRET has evolved to become a potent method of studying protein-protein interactions and also, increasingly, dynamic conformational changes within proteins (28, 29). To study G protein–coupled receptor signaling, sensors for receptor and G protein activation (30–33) as well as for the detection of various second messengers have been developed (34, 35). To determine the degree of activation of the β_1-AR in living cells in real time, we measured FRET between a mutant cyan fluorescent protein, Cerulean (Cer), fused to the carboxy terminus of the human β_1-AR and a yellow fluorescent protein (YFP) inserted into the third intracellular loop. A comparison of the activation characteristics of the 2 frequently occurring receptor polymor-

Nonstandard abbreviations used: β-AR, β-adrenergic receptor; Cer, Cerulean: cyan-emitting variant of GFP; CFP, cyan fluorescent protein; EC_{50}, half-maximal effective concentration; FlAsH, fluorescein arsenical hairpin binder; FRET, fluorescent resonance energy transfer; Iso, isoproterenol; NE, norepinephrine; YFP, yellow fluorescent protein.

Conflict of interest: The authors have declared that no conflict of interest exists.

Citation for this article: *J. Clin. Invest.* **117**:229–235 (2007). doi:10.1172/JCI30012.

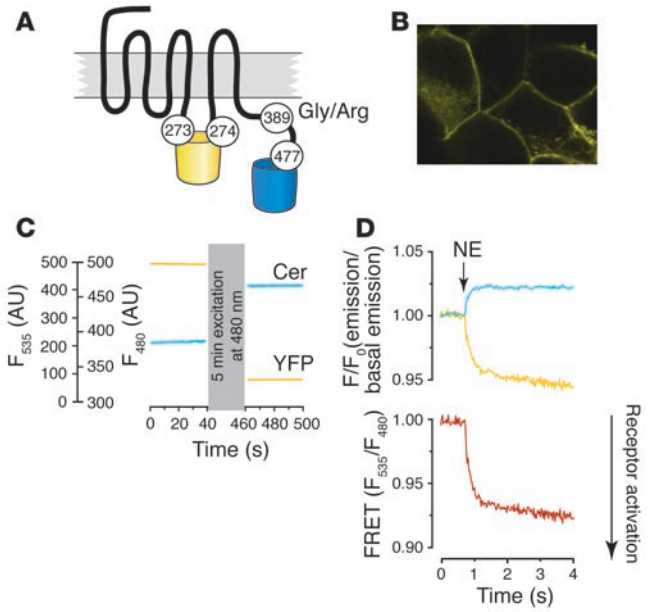

Figure 1
Development of a β_1-AR–FRET sensor. (**A**) Overall transmembrane topology of recombinant β_1-AR (Gly/Arg389–β_1-AR sensor) constructs. Using a linker (GlyGlyGlyGlyGly), we fused the cDNA encoding the Cerulean variant of GFP (Cer, blue) (49) to the carboxy terminus of the β_1-AR (position 477). YFP (yellow) was introduced into the third intracellular loop of the β_1-AR at position 273. (**B**) Visualization of transiently expressed β_1-AR sensor in HEK293 cells by confocal microscopy. Original magnification, ×63. (**C**) Effect of photobleaching. Emission intensities of YFP (535 nm, yellow) and Cerulean (Cer, 480 nm, blue) were recorded simultaneously from single cells expressing β_1-AR sensor using fluorescence microscopy. Emission intensities were recorded before and after the acceptor fluorophore was photobleached by 5 minutes exposure to light at 480 nm. (**D**) Time-resolved changes of the FRET ratio F_{535}/F_{480} in single HEK293 cells expressing the β_1-AR sensor. Emission intensities of YFP (535 nm, yellow trace), Cer (480 nm, blue trace), and the FRET ratio F_{535}/F_{480} (red trace) were recorded simultaneously from single cells. The decrease in FRET ratio is representative of the activation of the β_1-AR. The small arrow indicates the start of superfusion of the cell with 10 μM NE.

phisms Arg389 and Gly389 revealed substantial differences in the response of these receptor variants to beta blockers.

Results

Functional characterization of the β_1-AR–FRET sensor. We generated a mutant β_1-AR into which the cyan- and yellow-emitting variants of GFP (Cer and YFP) were inserted at the C terminus and in the third intracellular loop of the receptor, respectively. This FRET receptor construct is referred to as the β_1-AR sensor (Figure 1A). Confocal microscopy showed that the β_1-AR sensor was well expressed and targeted to the cell membrane (Figure 1B). Signals recorded from single HEK293 cells expressing the β_1-AR sensor were then analyzed at emission wavelengths of 480 nm (Cer) and 535 nm (YFP) upon excitation at 436 nm (Cer excitation). Excitation at 436 nm resulted in significant emission at 535 nm, characteristic for FRET. Bleaching of the acceptor YFP with intense light at 480 nm, resulting in an 80% reduction of the 535 nm emission, caused an increase of the emission at 480 nm of 20%, indicating that the emission at 535 nm was indeed due to FRET (Figure 1C). The ratio F_{535}/F_{480}, where F_{535} and F_{480} are the emission intensities at 535 nm and 480 nm, respectively (corrected for spillover and direct excitation of YFP; refs. 30, 33), was used in subsequent experiments as a measure of FRET. We then investigated the effect of the endogenous agonist norepinephrine (NE) on the FRET signal of the β_1-AR sensor. Superfusion of transiently transfected HEK293 cells with 10 μM NE led to a simultaneous increase in Cer emission and decrease in YFP emission. This amounted to an average decrease of the F_{535}/F_{480} FRET ratio by approximately 4% (Figure 1D). This loss of FRET reflects the agonist-induced receptor activation, as has been described for other receptor constructs (33, 36, 37) (Figure 1D).

We then investigated in detail how closely the β_1-AR–FRET sensor reflected the pharmacological and signaling characteristics of the wild-type receptor. Concentration-response curves of β_1-AR sensor activation for NE and isoproterenol (Iso) yielded half-maximal effective concentration (EC_{50}) of 1.8 ± 0.2 μM and 230 ± 40 nM, respectively (Figure 2A), which is similar to the wild-type receptor characteristics (K_i [NE] 3.6 μM; K_i [Iso] 220 nM) (38). The fast agonist-induced decrease of the FRET signal corresponding to activation of the receptor was rapidly and completely reversed upon application of the receptor antagonist propranolol. Propranolol had no effect on the basal FRET signal when it was applied alone (Figure 2B). Finally, we tested the capacity of the β_1-AR sensor to induce production of cAMP. HEK293 cells were cotransfected with the FRET-based cAMP sensor Epac1-camps and the β_1-AR sensor or with the unlabeled β_1-AR. To block endogenously expressed β_2-ARs, β_1-AR activation with Iso (1 nM) was carried out in the presence of the specific β_2-AR antagonist ICI 118551 (200 nM). We then determined FRET of Epac1-camps, which corresponds to cAMP production (34). As shown in Figure 2C, induction of cAMP production through the β_1-AR sensor closely resembled the signal of the unlabeled receptor with respect to both the kinetics and the extent of cAMP formation. This FRET signal must be entirely due to the cAMP sensor, as 1 nM Iso does not lead to detectable activation of the β_1-AR sensor (see Figure 2A) and also because the cAMP sensor is expressed at higher levels throughout the cytosol and yields a much higher FRET response compared with the β_1-AR sensor. To assess the expression levels of the 2 sensors, we used the YFP signal of Epac1-camps–expressing cells as compared with β_1-AR sensor–expressing cells (Epac1-camps YFP signal versus β_1-AR sensor YFP signal, 440 ± 460 versus 2290 ± 320 AU; n = 6 and 7, respectively). Together, these data indicate that the β_1-AR sensor is properly targeted to the cell surface and retains essential binding and signaling properties of the unlabeled receptor.

Dynamics of receptor conformational changes. Determination of FRET signals from single cells after agonist stimulation allowed the analysis of the activation kinetics of the β_1-AR (Figure 2, D and E). Under all conditions, the decrease of the FRET ratio followed a monoexponential time course and was thus fitted to the equation $f(t) = A(1 - e^{-t/\tau})$, ($e$ is the number of Euler) where $f(t)$ is function of time, A is the magnitude of the signal, and τ is the time constant. Consistent with the law of mass action, increasing concentrations of agonist resulted in shorter activation times (Figure 2E). As shown in Figure 2E, under saturating conditions, the β_1-AR is activated with a time constant of about 60 ms. To deter-

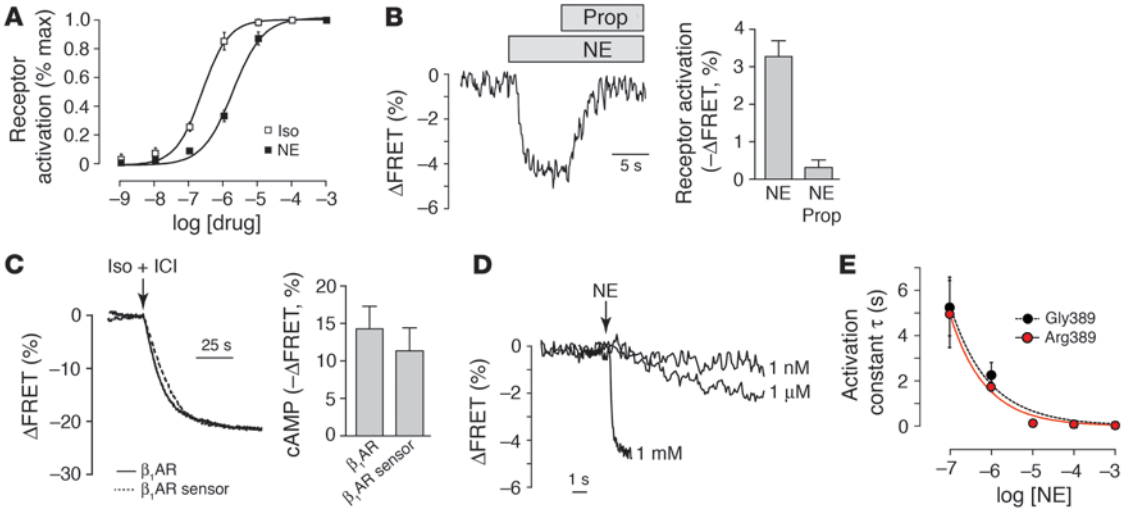

Figure 2

Characterization of the FRET sensor. (**A**) Concentration-response relation for the change in FRET in response to NE (filled squares) and Iso (open squares) in cells expressing the β_1-AR sensor (n = 4–6 per concentration and per group). (**B**) FRET signal caused by NE (10 μM; n = 10) is reversible by addition of the antagonist propranolol (Prop, 10 μM; n = 10) in HEK293 cells transiently expressing the β_1-AR sensor. (**C**) Comparison between the signaling properties of the β_1-AR sensor (n = 6) and the respective unlabeled receptor (n = 5) transiently expressed in HEK293 cells. cAMP detection was achieved using the Epac1-camps FRET sensor, and specific β_1-adrenergic stimulation was carried out by simultaneous application of ISO (1 nM) and the specific β_2-AR antagonist ICI 118551 (ICI; 200 nM). (**D**) Time-resolved changes in the FRET ratio F_{535}:F_{480} of the β_1-AR sensor transiently expressed in HEK293 cells at various concentrations of NE. (**E**) Relationship between time activation constant (τ) and agonist concentration for the Gly389–β_1-AR sensor (filled circles; n = 6–14 per concentration) and for the Arg389–β_1-AR sensor (red circles; n = 5–8 per concentration). At low concentrations of agonist, τ values were directly proportional to the agonist concentration whereas at higher concentrations of agonist, the values approached a maximum of 60 ms. The Arg389 polymorphism did not affect the kinetics of receptor activation.

mine whether the presence of YFP in the third intracellular loop of the receptor limits the speed of the conformational change, we generated a second β_1-AR sensor (β_1-AR–FlAsH) in which a short sequence of 6 amino acids (CCPGCC) was inserted into the third intracellular loop instead of YFP. This sequence specifically binds a small molecule (fluorescein arsenical hairpin binder, FlAsH) that becomes highly fluorescent after binding and allows the detection of FRET between Cer and FlAsH (36, 39). The FlAsH-based β_1-AR sensor also responded with a decrease of the FRET ratio and a similar time constant of receptor activation (57 ± 3 ms; n = 4) in response to agonist activation, suggesting sterically unhindered receptor activation kinetics of the β_1-AR sensor (data not shown).

Receptor polymorphisms' impact on receptor conformational changes. To assess the potential role of the naturally occurring Arg389 variants of the β_1-AR in receptor activation, we generated an Arg389–β_1-AR sensor by point mutating position 389 of the β_1-AR sensor from glycine to arginine (see Figure 1A). Upon expression in HEK293 cells, both the Gly389–β_1-AR sensor and the Arg389–β_1-AR sensor showed equal expression levels as determined by radioligand binding (Gly389 versus Arg389, 2.1 ± 0.3 versus 2.2 ± 0.2 pmol/mg membrane protein; n = 4) as well as equal YFP intensity (Gly389 versus Arg389, 2292 ± 316 versus 2052 ± 183 AU; n = 7 and 9, respectively). The Arg389 variant displayed a slightly increased sensitivity to NE (EC_{50} [Arg389]: 0.85 ± 0.1 μM; EC_{50} [Gly389]: 1.83 ± 0.25 μM; Supplemental Figure 1A; supplemental material available online with this article; doi:10.1172/JCI30012DS1), with nearly identical time constants of activation for the 2 receptor variants (Figure 2E). NE and Iso induced similar changes in the receptor FRET signal (Supplemental Figure 1B) as well as cAMP formation (Supplemental Figure 1C) for the 2 receptor variants. This was not due to saturation of the Epac1 sensor, as adenylyl cyclase activation and phosphodiesterase inhibition significantly enhanced cAMP levels even after stimulation of the β_1-AR with a high concentration of Iso (100 nM) (Supplemental Figure 2A). In addition, we studied coupling of the β_1-AR to Gs. Again, we used a FRET-based approach based on a YFP-labeled G protein αs subunit, a cyan fluorescent protein (CFP)-labeled γ_2 subunit, and a nonlabeled β_1 subunit (30, 40) (Supplemental Figure 1D). HEK293 cells transfected with the unlabeled Gly389–β_1-AR or Arg389–β_1-AR and with Gαs-YFP, Gβ, and Gγ-CFP, respectively, were simultaneously stimulated with NE (100 μM) plus ICI 118551 (200 nM) to block β_2-ARs. No difference in β_1-AR–mediated Gs activation was observed between the 2 receptor variants (Supplemental Figure 1D). In addition, we determined the basal (i.e., in the absence of agonist) cAMP levels that the 2 receptor variants generated. Both variants exhibited the same basal Epac1-FRET signal calculated from cells expressing the Epac1-camps and the unlabeled β-AR receptor variants (Supplemental Figure 2B). Moreover, we assessed the maximal cAMP-generating capacity of the 2 receptor variants. To this end, we treated Gly389–β_1-AR transfected cells and Arg389–β_1-AR transfected cells with forskolin and the phosphodiesterase inhibitor IBMX (100 μM) (Supplemental Figure 2C). Both cell lines exhibited very similar maximal cAMP levels, confirming our previous notion (the validity of cAMP determination; see Supplemental Figure 2B) that the 2 receptor variants do not differ significantly with respect to their basal constitutive activity in terms of whole cell cAMP generation.

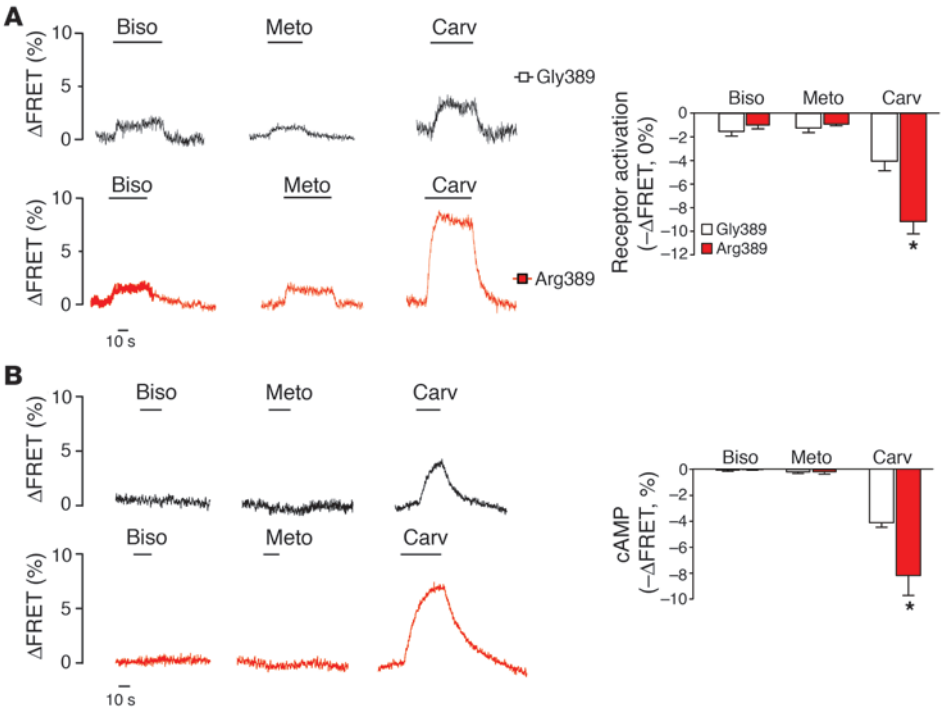

Figure 3
Impact of receptor polymorphisms. (**A**) Receptor activation in cells expressing the Gly389–β_1-AR sensor (white bars) or the Arg389–β_1-AR sensor (red bars) after beta blocker application (100 μM metoprolol, bisoprolol, or carvedilol) (n = 5–13 per group). (**B**) Effects of beta blockers (100 μM) on cAMP levels in cells expressing the unlabeled Gly389–β_1-AR (white bars) or the Arg389–β_1-AR (red bars) (n = 8–12 per group). *P < 0.05, statistically significant differences. Biso, bisoprolol; meto, metoprolol; carv, carvedilol.

We then compared the FRET signals of the 2 variants due to several antagonists currently in clinical use (Figure 3). In contrast with the agonist, which induced a decrease in the FRET ratio, bisoprolol, metoprolol, and carvedilol led to an increase in the FRET ratio, i.e., an active change of the receptor conformation, suggesting inverse agonist behavior (37). Upon washout, the signals induced by these compounds were slowly reversed, which was compatible with their high affinity to the receptor and, consequently, slow dissociation. As equilibrium conditions regarding ligand receptor interactions cannot be reached within a feasible time frame for low ligand concentrations (Figure 2D), high concentrations of β-AR antagonists were studied. Compared with the modest increases of the β_1-AR–FRET signal induced by bisoprolol and metoprolol, carvedilol induced a more than 2-fold greater increase of the FRET signal of the Gly389–β_1-AR (Figure 3A). The 389-receptor polymorphism did not affect the response to metoprolol and bisoprolol, whereas Arg389-receptors responded more than 2-folds stronger to carvedilol than they did to metoprolol and bisoprolol.

The differences observed at the receptor level became even more pronounced at the level of the second messenger cAMP, as measured with the cAMP sensor. Whereas bisoprolol and metoprolol induced no decreases of cAMP, carvedilol led to a marked reduction of basal cAMP (Figure 3B), and again, the Arg389 variant of the β_1-AR led to a much stronger basal cAMP reduction.

Studies in primary cardiomyocytes. We next studied the impact of the 389 polymorphism on cardiac rate control in primary cardiac myocytes (Figure 4). We employed adenoviral gene transfer to express equal levels of the 2 variants of the β_1-AR in primary rat cardiac myocytes (2.7 ± 0.2 pmol/mg for the Gly389 variant and 2.8 ± 0.4 pmol/mg for the Arg389 variant; n = 4 per group). Expression of the Arg389 variant led to a higher beating frequency compared with the Gly389 variant already under basal conditions. Cardiac myocytes carrying the Arg389 variant, but not those carrying the Gly389 variant of the β_1-AR, responded to the treatment with carvedilol (1 μM) with a significant reduction (25%) of the beating frequency. The absence of an effect of carvedilol on Gly389-transfected cardiomyocytes is in line with data examining cAMP formation after lower concentrations of carvedilol (data not shown). Under these conditions, only the Arg389, and not Gly389, of the β_1-AR, responded with a decrease of cAMP.

Discussion

The β-AR has served as a prototypical receptor in the study of cellular signaling mediated by G protein–coupled receptors (41). Despite this receptor being among the most intensely studied G protein–coupled receptors, it has not been possible to assess the activation of the β_1-AR in a direct manner. Recently, the use of GFP-based FRET has allowed the direct optical recording of G protein–coupled receptor activation (33). Here, we have applied this technology to the human β_1-AR.

This first direct determination of conformational changes of the β_1-AR in living cells revealed several critical characteristics of this GPCR. The β_1-AR is activated at a high speed of approximately 60 ms, thereby resembling several neurotransmitter receptors (33, 36). We provide direct evidence that some beta blockers can induce a very distinct receptor conformation compared to that induced by agonists, which is compatible with inverse agonism at the β_1-AR. Of clinical relevance, the 2 most frequent variants of the β_1-AR (Gly389, 26% allele frequency, and Arg389, 74% allele frequency; ref. 10) differ dramatically in their response to beta blocker treatment, with the Arg389 variant being exquisitely sensitive to carvedilol.

We have investigated whether our β_1-AR–FRET sensor truly retained the behavior of the native receptor. Multiple lines of evidence indicate that this is the case. The β_1-AR sensor was properly targeted to the cell membrane; the vast majority of the FRET signal recorded thus derives from receptors in their native environment. The modified receptors displayed ligand binding affinities similar to those of the unlabeled receptor (38), and their signaling

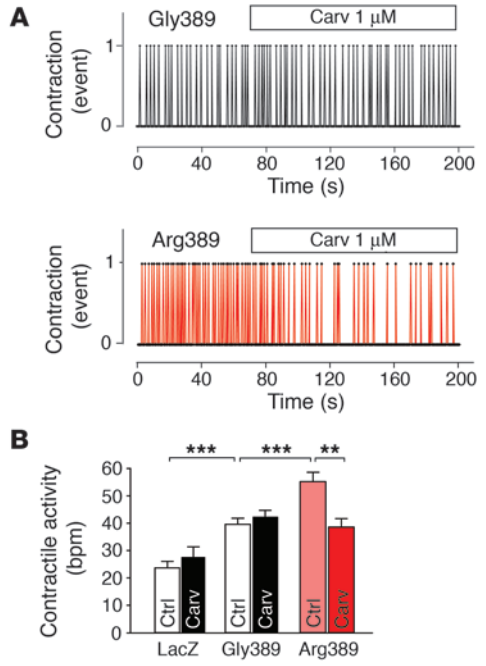

Figure 4

Supersensitivity of the Arg389–β_1-AR polymorphism to carvedilol. (**A**) Representative tracings of the beating frequency of cardiomyocytes infected with the Gly389–β_1-AR sensor or the Arg389–β_1-AR sensor before and after stimulation with carvedilol (1 μM). The number of beats per minute was determined from the digitized video images by an observer who was blinded to the experimental protocol. (**B**) Effect of carvedilol (1 μM) on the beating frequency of cardiomyocytes infected with LacZ, the Gly389–β_1-AR sensor, or the Arg389–β_1-AR sensor (5 independent cardiomyocyte isolations each, including 5–10 measurements for each of the 6 groups). $^{**}P < 0.01$ and $^{***}P < 0.001$, statistically significant differences. Ctrl, control.

was entirely normal. As an additional control, to rule out the possibility that the activation kinetics of the receptor were not limited by the insertion of YFP into the third intracellular loop, we constructed a β_1-AR sensor, where the YFP was replaced by a 6–amino acid sequence, which allows the binding of a small fluorescent dye (FlAsH). FRET-based analysis of the activation kinetics of this FlAsH receptor showed exactly the same characteristics as the original β_1-AR sensor, effectively excluding a significant influence of the YFP located in the third intracellular loop. Taken together, our results demonstrate that our FRET sensors retain the essential properties of the parent β_1-AR.

The ability to directly assess the activation of the human β_1-AR was then employed to determine the effects of clinically used beta blockers on the receptor protein itself and on downstream signal transduction. Beta blockers are among the most effective therapeutic agents for the treatment of common cardiovascular disorders, such as hypertension, coronary artery disease, and heart failure (8). Three different substances (bisoprolol, carvedilol, and metoprolol) are currently used for the treatment of heart failure, and there is an ongoing debate over whether these substances differ as to their effectiveness and, if so, what the molecular basis of such differences might be (8). Based on second messenger data or complex parameters, such as force of contraction of isolated myocardial tissue, inverse agonist properties have been suggested by some and disputed by others (38, 42–44). The β_1-AR–FRET sensor allowed, for what we believe is the first time, the direct assessment of the effects of various β_1-AR antagonists on receptor conformational changes. We observed that all antagonists studied induced conformational changes (increase of FRET signal) opposite to those of agonist effects, indicating that this differential movement of different receptor domains after ligand binding represents the molecular basis for agonism and inverse agonism at the β_1-AR. Interestingly, the atypical beta blocker carvedilol was markedly more effective than metoprolol and bisoprolol both in inducing the inverse agonist conformation of the receptor protein and in decreasing basal cAMP levels.

These findings are in agreement with respect to the effect of carvedilol on heart rate control in Gly389–β_1-AR–expressing mice (45) as well as cAMP-formation in Gly389–β_1-AR–expressing cells (38). Inverse agonistic properties have been described for metoprolol and bisoprolol, which we cannot confirm with the present study (42, 44). Two recent studies assessed the impact of the 389 polymorphism on cardiac function in heart failure patients. While one study associated the Arg389 polymorphism with the beneficial effects of carvedilol (15), a second study found no significant association (46).

However, these studies often investigated very complex systems, such as human tissue with highly variable catecholamine concentrations from heart failure patients, tissue from patients with unknown receptor polymorphism status, and cell lines or transgenic mice with long-term overexpression of the β-AR. In contrast, our current study is the first, to our knowledge, to directly assess the impact of various beta blockers on the conformational change of the β_1-AR.

This study identified a unique property of carvedilol, which is likely to become clinically relevant. When we directly assessed how the most frequent receptor polymorphism influenced intrinsic properties of receptor activation, we found a dramatic hypersensitivity of the Arg389 variant to carvedilol. The Arg389 variant of the human β_1-AR, which is present in the majority of individuals, displayed a 2-fold greater response to carvedilol than the so-called wild-type Gly389, which really is the second most frequent 389 variant. This pronounced change in receptor conformation transduced into downstream functional effects, as we found in experiments determining myocyte beating rate. In this physiologically relevant model, we also saw an enhanced beating frequency in cells expressing the Arg389 variant of the β_1-AR under basal conditions, which is in line with a previous study (10). Thus, while we did not find a significantly enhanced capacity of the Arg389–β_1-AR variant to form cAMP under basal conditions in HEK cells (Supplemental Figure 2), expression of the 2 receptor variants in primary rat cardiomyocytes revealed differences as to their chronotropic effect. This is most likely due to the cardiomyocyte environment, where localized submembrane cAMP has been shown to regulate channel activity (47, 48), but cannot yet be resolved by Epac1-camps determination.

Both metoprolol and bisoprolol did not markedly affect cAMP of Arg389-β_1-AR–expressing cells. Thus, carvedilol appears to be unique in its ability to suppress the chronically enhanced basal signaling of the Arg389 variant of the β_1-AR. This finding is potentially of great clinical importance, as the presence of the Arg389 polymorphism has been suggested as determining a poor prognosis in heart failure patients.

The present data show, for what we believe is the first time, real-time measurements of β_1-AR activation in living cells and provide

evidence for supersensitivity of the frequent Arg389 variant of the β_1-AR toward carvedilol. It will be interesting to investigate whether patients carrying the Arg389 polymorphism may benefit most from treatment with carvedilol as opposed to other beta blockers.

Methods

Molecular biology and cell culture. Constructions of recombinant β_1-ARs (β_1-AR sensor and β_1-AR–FlAsH) were performed using Pfu DNA polymerase (Stratagene). Using a linker (GlyGlyGlyGlyGly), we fused the Cer variant of GFP (49) to the carboxy terminus of the β_1-AR (AA 477). YFP (or the CCPGCC motif for FlAsH) was introduced into the third intracellular loop of the β_1-AR at position 273. Site-directed mutagenesis at position 389 following a PCR strategy was carried out to generate the Arg389–β_1-AR sensor construct (QuikChange II Site-Directed Mutagenesis kit; Stratagene). All constructs were verified by sequencing and subcloned into pTREXdest30 (Invitrogen) for eukaryotic expression. Unlabeled (Arg389–β_1-AR and Gly389–β_1-AR) and the sensor constructs of the β_1-AR receptor, Epac1-camps (34), YFP-labeled G protein αs subunit (50) (kindly provided by C. Berlot, Weiss Center for Research, Geisinger Clinic, Danville, Pennsylvania, USA), CFP-labeled G protein γ_2 subunit (51), and G protein β_1 subunit were expressed transiently by transfection using Effectene (QIAGEN) in HEK293 cells.

FRET measurements. Cells were split 24 hours after transfection and seeded on polylysine-coated coverslips. Cells were kept in culture for an additional 24 hours. For the FlAsH–β_1-AR construct, FlAsH labeling was carried out on the day of the experiment as described (36). Cells grown on coverslips were then maintained at room temperature in the FRET buffer (140 mM NaCl, 4.5 mM KCl, 10 mM Hepes, 2 mM $CaCl_2$, 2 mM $MgCl_2$, pH 7.4). FRET experiments were performed using a Zeiss-inverted microscope (Axiovert 200) equipped with an oil-immersion ×63 objective and a dual-emission photometric system (TILL Photonics) equipped with a polychrome IV light source (TILL Photonics). FRET was monitored as the emission ratio of YFP to Cer, F_{535}/F_{480}, where F_{535} and F_{480} are the emission intensities at 535 ± 15 nm and 480 ± 20 nm (505 nm DCLP beam splitter) upon excitation at 436 ± 10 nm (beam splitter DCLP 455 nm). The emission ratio was corrected by the respective spillover of Cer into the 535 nm channel and the direct excitation of YFP at 436 nm. To determine whether intermolecular FRET arising from varying expression levels of the FRET sensors employed would influence our results, we reanalyzed our data and calibrated them for the YFP signal recorded from each cell, thereby normalizing for receptor expression. Calibration for receptor expression did not alter the results as compared with the original data. To determine pharmacological stimulation–induced FRET changes, cells were continuously superfused with FRET buffer, and ligands were applied using the computer-assisted solenoid valve–controlled rapid superfusion device ALA-VM (ALA Scientific Instruments; solution exchange 5–10 ms). Signals detected by amplified photodiodes (TILL Photonics) were digitalized using an analog digitizer converter (Digidata 1322A; Axon Instruments) and stored on a personal computer using Clampex 9.0 software (Axon Instruments). Carvedilol was from SmithKline Beecham; NE, Iso, ICI 118551, propranolol, and metoprolol-tartrate were from Sigma-Aldrich; and bisoprolol fumarate was from Merck.

Confocal microscopy. Confocal microscopy was performed using a Leica TCS SP2 system with an Attofluor holder (Invitrogen). YFP was excited with the 514-nm line of an argon laser, and images were taken with a ×63 objective using the factory settings for YFP fluorescence (530–600 nm).

Adenovirus generation. Recombinant adenoviral vectors were generated according to standard procedures. Gly389–β_1-AR sensor and Arg389–β_1-AR sensor were amplified by PCR and introduced into adenoviral vectors (pAD/CMV/V5-DEST; Invitrogen) by homologous recombination. A corresponding LacZ-expressing adenoviral vector (pAd/CMV/LacZ) was used as control. Adenovirus titers were determined by plaque assays in HEK293 monolayer cultures embedded in agarose.

Cardiomyocyte isolation, adenoviral transfection, and contractile activity. Neonatal cardiomyocytes were isolated from hearts of 1- to 2-day-old Sprague Dawley rats by enzymatic digestion essentially as described previously (52). Cardiomyocytes were plated on 96-well plates in medium containing 5% FCS. After 24 hours, medium was replaced by 1% FCS medium, and adenoviral transfection was performed at an MOI of 50. Contractile activity of cardiomyocytes was monitored 48 hours after infection. Live cells were held thermostatically at 32°C and examined under a microscope with a ×63 oil-immersion objective; bright field images were recorded every 400 ms, and the number of beats per minute was determined from the digitized video images. Beating frequency was determined before and after pharmacological stimulation by an observer who was blinded to the experimental protocol. Cardiomyocyte contractility was measured using edge detection perpendicular to the outward cell edge using MetaMorph software (Visitron Systems). Contraction events were defined based on the inward movement (≥ 5 pixels, corresponding to 0.510 μM) of the cell edge toward the nucleus, resulting in a digital information of cell contractility.

Membrane preparation and radioligand-binding assays. Transfected HEK293 cells, infected cardiomyocytes, or native cells were washed with PBS, and membrane fractions were prepared as described (53). The resulting membrane pellets were resuspended in 50 mM Tris buffer, pH 7.4. Protein concentrations were determined by the Bradford method using bovine serum albumin (Sigma-Aldrich) as standard. Radioligand-binding experiments were performed in 50 mM Tris-HCl, pH 7.4, in the presence of 100 μM GTP to ensure monophasic competition curves for agonists (38). For competition binding experiments, we used 50 pM ^{125}I-CYP. Nonspecific binding was determined in the presence of 10 μM alprenolol.

Statistics. Average data are presented as mean ± SEM. Statistical analysis was carried out using the Prism software package (version 4.0; GraphPad Software). Statistical significance was evaluated by unpaired 2-tailed Student's *t* test. $P < 0.05$ was considered statistically significant.

Acknowledgments

These studies were funded by the Rudolf-Virchow-Center/DFG–Research Center for Experimental Biomedicine, supported by the Deutsche Forschungsgemeinschaft, ProCorde/Trigen, Sanofi-Aventis, and the Bavarian Ministry of Economics. We would like to thank the Foundation Leducq for generously supporting this project. F. Rochais was supported by a fellowship of the Bayerische Forschungsstiftung. The expert technical assistance of Silke Oberdorf-Maass, Nadine Hemmrich, and Ursula Keller is gratefully acknowledged. We would like to thank Gisbert Sponer for advice on carvedilol and Carsten Hoffmann for advice on FlAsH.

Received for publication August 9, 2006, and accepted in revised form November 7, 2006.

Address correspondence to: Stefan Engelhardt, Rudolf-Virchow-Center, DFG–Research Center for Experimental Biomedicine, University of Würzburg, Versbacher Strasse 9, 97078 Würzburg, Germany. Phone: 49-931-201-48710; Fax: 49-931-201-48539; E-mail: stefan.engelhardt@virchow.uni-wuerzburg.de.

Jean-Pierre Vilardaga's present address is: Simches Research Center, Program in Membrane Biology, Massachusetts General Hospital and Harvard Medical School, Boston, Massachusetts, USA.

1. Brodde, O.E., and Michel, M.C. 1999. Adrenergic and muscarinic receptors in the human heart. *Pharmacol. Rev.* **51**:651–690.
2. Thom, T., et al. 2006. Heart disease and stroke statistics–2006 update: a report from the American Heart Association Statistics Committee and Stroke Statistics Subcommittee. *Circulation.* **113**:e85–e151.
3. Cohn, J.N., et al. 1984. Plasma norepinephrine as a guide to prognosis in patients with chronic congestive heart failure. *N. Engl. J. Med.* **311**:819–823.
4. Freedman, N.J., and Lefkowitz, R.J. 2004. Anti-β_1-adrenergic receptor antibodies and heart failure: causation, not just correlation. *J. Clin. Invest.* **113**:1379–1382. doi:10.1172/JCI200421748.
5. Lohse, M.J., Engelhardt, S., and Eschenhagen, T. 2003. What is the role of β-adrenergic signaling in heart failure? *Circ. Res.* **93**:896–906.
6. Engelhardt, S., Hein, L., Wiesmann, F., and Lohse, M.J. 1999. Progressive hypertrophy and heart failure in β_1-adrenergic receptor transgenic mice. *Proc. Natl. Acad. Sci. U. S. A.* **96**:7059–7064.
7. Black, J.W., and Stephenson, J.S. 1962. Pharmacology of a new adrenergic β-receptor-blocking compound (Nethalide). *Lancet.* **2**:311–314.
8. Bristow, M. 2003. Antiadrenergic therapy of chronic heart failure: surprises and new opportunities. *Circulation.* **107**:1100–1102.
9. Maqbool, A., Hall, A.S., Ball, S.G., and Balmforth, A.J. 1999. Common polymorphisms of β_1–adrenoceptor: identification and rapid screening assay. *Lancet.* **353**:897.
10. Mason, D.A., Moore, J.D., Green, S.A., and Liggett, S.B. 1999. A gain-of-function polymorphism in a G-protein coupling domain of the human β_1-adrenergic receptor. *J. Biol. Chem.* **274**:12670–12674.
11. Small, K.M., Wagoner, L.E., Levin, A.M., Kardia, S.L., and Liggett, S.B. 2002. Synergistic polymorphisms of β_1- and α_{2C}-adrenergic receptors and the risk of congestive heart failure. *N. Engl. J. Med.* **347**:1135–1142.
12. Eason, M.G., and Liggett, S.B. 1996. Chimeric mutagenesis of putative G-protein coupling domains of the α_{2A}-adrenergic receptor. Localization of two redundant and fully competent Gi coupling domains. *J. Biol. Chem.* **271**:12826–12832.
13. O'Dowd, B.F., et al. 1988. Site-directed mutagenesis of the cytoplasmic domains of the human β_2-adrenergic receptor. Localization of regions involved in G protein-receptor coupling. *J. Biol. Chem.* **263**:15985–15992.
14. Palczewski, K., et al. 2000. Crystal structure of rhodopsin: a G protein-coupled receptor. *Science.* **289**:739–745.
15. Mialet Perez, J., et al. 2003. β_1-Adrenergic receptor polymorphisms confer differential function and predisposition to heart failure. *Nat. Med.* **9**:1300–1305.
16. Bengtsson, K., et al. 2001. Polymorphism in the β_1-adrenergic receptor gene and hypertension. *Circulation.* **104**:187–190.
17. Brodde, O.E., and Stein, C.M. 2003. The Gly389Arg β_1-adrenergic receptor polymorphism: a predictor of response to β-blocker treatment? *Clin. Pharmacol. Ther.* **74**:299–302.
18. Small, K.M., McGraw, D.W., and Liggett, S.B. 2003. Pharmacology and physiology of human adrenergic receptor polymorphisms. *Annu. Rev. Pharmacol. Toxicol.* **43**:381–411.
19. Lohse, M.J. 2004. β-Adrenoceptor polymorphisms and heart failure. *Trends Mol. Med.* **10**:55–58.
20. Bruck, H., et al. 2005. The Arg389Gly β_1-adrenoceptor polymorphism and catecholamine effects on plasma-renin activity. *J. Am. Coll. Cardiol.* **46**:2111–2115.
21. Johnson, J.A., et al. 2003. β_1-Adrenergic receptor polymorphisms and antihypertensive response to metoprolol. *Clin. Pharmacol. Ther.* **74**:44–52.
22. Liu, J., et al. 2003. Gly389Arg polymorphism of β_1-adrenergic receptor is associated with the cardiovascular response to metoprolol. *Clin. Pharmacol. Ther.* **74**:372–379.
23. Sofowora, G.G., et al. 2003. A common β_1-adrenergic receptor polymorphism (Arg389Gly) affects blood pressure response to β-blockade. *Clin. Pharmacol. Ther.* **73**:366–371.
24. Terra, S.G., et al. 2005. β_1-Adrenergic receptor polymorphisms and left ventricular remodeling changes in response to β-blocker therapy. *Pharmacogenet. Genomics.* **15**:227–234.
25. Joseph, S.S., Lynham, J.A., Grace, A.A., Colledge, W.H., and Kaumann, A.J. 2004. Markedly reduced effects of (-)-isoprenaline but not of (-)-CGP12177 and unchanged affinity of β-blockers at Gly389-β_1-adrenoceptors compared to Arg389-β_1-adrenoceptors. *Br. J. Pharmacol.* **142**:51–56.
26. Molenaar, P., et al. 2002. Conservation of the cardiostimulant effects of (-)-norepinephrine across Ser49Gly and Gly389Arg β_1-adrenergic receptor polymorphisms in human right atrium in vitro. *J. Am. Coll. Cardiol.* **40**:1275–1282.
27. O'Shaughnessy, K.M., Fu, B., Dickerson, C., Thurston, D., and Brown, M.J. 2000. The gain-of-function G389R variant of the β_1-adrenoceptor does not influence blood pressure or heart rate response to β-blockade in hypertensive subjects. *Clin. Sci. (Lond.).* **99**:233–238.
28. Förster, T. 1948. Zwischenmolekulare Energiewanderung und Fluoreszenz [abstract]. *Annals of Physics (Leipzig).* **2**:55–75.
29. Miyawaki, A. 2003. Visualization of the spatial and temporal dynamics of intracellular signaling. *Dev. Cell.* **4**:295–305.
30. Bunemann, M., Frank, M., and Lohse, M.J. 2003. Gi protein activation in intact cells involves subunit rearrangement rather than dissociation. *Proc. Natl. Acad. Sci. U. S. A.* **100**:16077–16082.
31. Gales, C., et al. 2005. Real-time monitoring of receptor and G-protein interactions in living cells. *Nat. Methods.* **2**:177–184.
32. Hein, P., Frank, M., Hoffmann, C., Lohse, M.J., and Bunemann, M. 2005. Dynamics of receptor/G protein coupling in living cells. *EMBO J.* **24**:4106–4114.
33. Vilardaga, J.P., Bunemann, M., Krasel, C., Castro, M., and Lohse, M.J. 2003. Measurement of the millisecond activation switch of G protein-coupled receptors in living cells. *Nat. Biotechnol.* **21**:807–812.
34. Nikolaev, V.O., Bunemann, M., Hein, L., Hannawacker, A., and Lohse, M.J. 2004. Novel single chain cAMP sensors for receptor-induced signal propagation. *J. Biol. Chem.* **279**:37215–37218.
35. Nikolaev, V.O., Gambaryan, S., and Lohse, M.J. 2006. Fluorescent sensors for rapid monitoring of intracellular cGMP. *Nat. Methods.* **3**:23–25.
36. Hoffmann, C., et al. 2005. A FlAsH-based FRET approach to determine G protein-coupled receptor activation in living cells. *Nat. Methods.* **2**:171–176.
37. Vilardaga, J.P., Steinmeyer, R., Harms, G.S., and Lohse, M.J. 2005. Molecular basis of inverse agonism in a G protein-coupled receptor. *Nat. Chem. Biol.* **1**:25–28.
38. Hoffmann, C., Leitz, M.R., Oberdorf-Maass, S., Lohse, M.J., and Klotz, K.N. 2004. Comparative pharmacology of human β-adrenergic receptor subtypes-characterization of stably transfected receptors in CHO cells. *Naunyn Schmiedebergs Arch. Pharmacol.* **369**:151–159.
39. Griffin, B.A., Adams, S.R., and Tsien, R.Y. 1998. Specific covalent labeling of recombinant protein molecules inside live cells. *Science.* **281**:269–272.
40. Hein, P., et al. 2006. Gs activation is time-limiting in initiating receptor-mediated signaling. *J. Biol. Chem.* **281**:33345–33351.
41. Rockman, H.A., Koch, W.J., and Lefkowitz, R.J. 2002. Seven-transmembrane-spanning receptors and heart function. *Nature.* **415**:206–212.
42. Varma, D.R., et al. 1999. Inverse agonist activities of β-adrenoceptor antagonists in rat myocardium. *Br. J. Pharmacol.* **127**:895–902.
43. Maack, C., et al. 2001. Characterization of β_1-selectivity, adrenoceptor-G(s)-protein interaction and inverse agonism of nebivolol in human myocardium. *Br. J. Pharmacol.* **132**:1817–1826.
44. Maack, C., et al. 2000. Different intrinsic activities of bucindolol, carvedilol and metoprolol in human failing myocardium. *Br. J. Pharmacol.* **130**:1131–1139.
45. Engelhardt, S., Grimmer, Y., Fan, G.H., and Lohse, M.J. 2001. Constitutive activity of the human β_1-adrenergic receptor in β_1-receptor transgenic mice. *Mol. Pharmacol.* **60**:712–717.
46. Liggett, S.B., et al. 2006. A polymorphism within a conserved β_1-adrenergic receptor motif alters cardiac function and β-blocker response in human heart failure. *Proc. Natl. Acad. Sci. U. S. A.* **103**:11288–11293.
47. Rochais, F., et al. 2006. A specific pattern of phosphodiesterases controls the cAMP signals generated by different Gs-coupled receptors in adult rat ventricular myocytes. *Circ. Res.* **98**:1081–1088.
48. Zhou, Y.Y., et al. 1997. Localized cAMP-dependent signaling mediates β_2-adrenergic modulation of cardiac excitation-contraction coupling. *Am. J. Physiol.* **273**:H1611–H1618.
49. Rizzo, M.A., Springer, G.H., Granada, B., and Piston, D.W. 2004. An improved cyan fluorescent protein variant useful for FRET. *Nat. Biotechnol.* **22**:445–449.
50. Hynes, T.R., Hughes, T.E., and Berlot, C.H. 2004. Cellular localization of GFP-tagged α subunits. *Methods Mol. Biol.* **237**:233–246.
51. Ruiz-Velasco, V., and Ikeda, S.R. 2001. Functional expression and FRET analysis of green fluorescent proteins fused to G-protein subunits in rat sympathetic neurons. *J. Physiol.* **537**:679–692.
52. Buitrago, M., et al. 2005. The transcriptional repressor Nab1 is a specific regulator of pathological cardiac hypertrophy. *Nat. Med.* **11**:837–844.
53. Klotz, K.N., et al. 1998. Comparative pharmacology of human adenosine receptor subtypes - characterization of stably transfected receptors in CHO cells. *Naunyn Schmiedebergs Arch. Pharmacol.* **357**:1–9.